Effect of Support Structure on Permeance of Thin Film Composite Membranes

Koushik Ponnuru[1], Lingxiang Zhu[1], Haiqing Lin[1] and Edward P. Furlani[1, 2]

Dept. of Chemical & Biological Engineering[1], Dept. of Electrical Engineering[2],
University at Buffalo (SUNY), Buffalo, NY 14260-4200, efurlani@buffalo.edu

ABSTRACT

An analysis is presented of the effects of support structure on the permeance of thin film composite membrane using an integral approach combining computational fluid dynamics simulations and experiments. 3D computational models are developed using COMSOL to systematically study the effects of the three key parameters (support porosity, support pore size and the thickness of the selective layer) on membrane permeance. The experimental results suggest that as the selective layer is produced thinner to enhance the water permeance, the geometric structure of the microporous support becomes more important. These findings are also consistent with the results from the computational models.

Keywords: Composite membrane, reverse osmosis (RO), microporous support, computational model.

1 INTRODUCTION

The production of potable water has become a worldwide concern to meet the demand of growing population.[1-3] Reverse osmosis (RO) membrane is the leading technology for desalination installations in producing drinkable water, due to high energy efficiency and resulting low costs. The popularization of RO membranes have been achieved by continual improvement in membrane separation performance and cost reduction. Fig. 1a shows a schematic of thin film composite membrane. The thin, dense skin layer (0.1 μm) performs molecular separation and the porous bulk of the membrane (150-200 μm) provides mechanical strength, but offers negligible resistance to mass transport for desalination.[1] However, as the selective layer is produced thinner to enhance the water permeance, the geometric structure of the microporous support becomes more important, because the porosity and pore size may restrict the concentration profile of the water in the selective layer, decreasing the penetrant permeance.[4, 5]

In this work, the membrane structure shown in Fig. 1 is simulated using a three-dimensional (3D) computational model. The membrane permeance is evaluated as a function of various membrane parameters including the thickness of the separating layer and the porosity and pore size of the microporous support. We have carried out a detailed parametric analysis and explored the complete design space to identify the parameter sets that can minimize the detrimental impact of the support and enhance the overall permeance of the composite membrane.

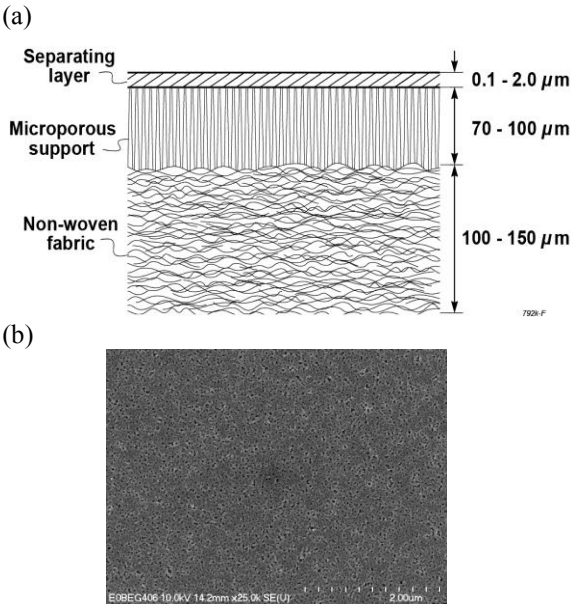

Fig. 1. (a) Schematic illustration of asymmetric thin film composite membrane for reverse osmosis desalination.[1] (b) Scanning electron micrograph on the surface of a microporous support membrane.

2 THEORY AND MODELING

The objective of this work is to understand and evaluate the effects of support geometrical features on the separation properties of thin film composite membranes. The steady state flux across the membrane is governed by various parameters including the diffusivity of the gas in the selective film and the support matrix, porosity and the pore size of the support matrix, thickness of the selective film, and the pressure of the feed and permeates. Fig. 2 shows the 3D computational model for the membrane structure shown in Fig. 1.

In this model, we make several assumptions to simplify the analysis, as shown below.

1. The species transporting through the membrane by diffusion is diluted; that is, the concentration is small compared to the solvent fluid.

(a)

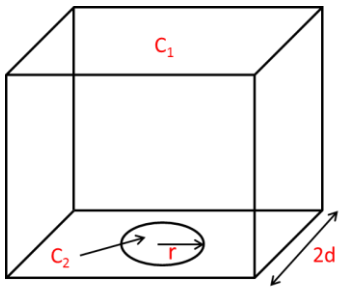

(b)

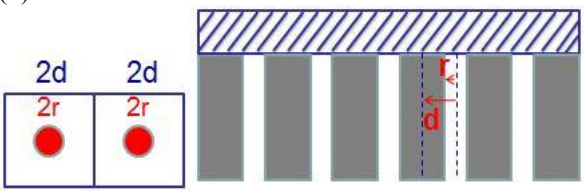

Fig.2. Geometry of (a) unit cell used for 3D model and (b) schematic drawing of composite membrane.

2. The support material is, for all practical considerations, impermeable; hence, the diffusivity of the support is taken as zero resulting in a no-flux condition.
3. Transport through the film is diffusive, and is therefore dictated by gradients in a chemical potential of the diffusing species, which may be water or salt. For conciseness of representation, the chemical potential is replaced here with a concentration.
4. The support pore is filled with water. So transport within the pore is convective and assumed to dominate over the diffusion within the film. The appropriate boundary condition under this assumption is that of a perfect sink, or zero concentration. Physically, this means that diffusing species reaching the interface are instantaneously removed.

The species transport within the membrane is governed by the fick's law of diffusion. Mass balance equation across the membrane:

$$\frac{\partial c}{\partial t} + u.\nabla c = \nabla.(D\nabla c) + R \qquad (1)$$

The above equation includes these quantities (with the SI unit in parentheses):

- c is the concentration of the species (mol/m3)
- D denotes the diffusion coefficient (m2/s)
- R is a reaction rate expression for the species (mol/(m^3·s))
- u is the velocity vector (m/s)

The first term on the left-hand side of Eq. (1) corresponds to the accumulation of the species. The second term accounts for the convective transport due to a velocity field u. On the right-hand side of the mass balance equation (Eq. (1)), the first term describes the diffusion transport, accounting for interaction between the dilute species and the solvent.

Thus, at steady-state this term goes to zero and the concentration field within the film reduces down to the following expression:

$$\nabla.(-D_i \nabla c_i) = 0 \qquad (2)$$

$$N_i = -D_i \nabla c_i \qquad (3)$$

To simplify the simulations, the concentration at the film/feed solution interface (C_1, as shown in Fig. 2a) is assumed to be 8.1 mol/m^3 (at a feed pressure of 2 atm), and the concentration at the film/pore interface (C_2) is 4.05 mol/m^3 (at a permeate pressure of 1 atm).

At the interface between the film and support material, the part of the bottom X–Y plane occupied by the support material, continuity of the flux requires:

$$D_f \frac{\partial C_f}{\partial Z} = D_s \frac{\partial C_s}{\partial Z} \qquad (4)$$

where D is the diffusion coefficient in the diffusing species within either the film or the support, here distinguished by the subscript f and s, respectively.

All the other exterior boundaries in the domain are left with the default no flux boundary condition, due to symmetry; no mass flows in or out of boundary, such that total flux is zero:

$$D_i.\nabla C_i = 0 \qquad (5)$$

An adaptive mesh function is used to ensure adequate refining of the mesh in the regions where the boundary condition transitions from a constant concentration to a no-flux condition. This has previously been shown to cause significant errors in the computation. Therefore, refinement is continued until the calculated solution became mesh-independent.

3 RESULTS AND DISCUSSION

The plots shown in the Figs. 3 and 4 represent the 3D concentration field for two different cases defined by a constant film thickness but different porosities of $\varepsilon = 0.2$ (Fig. 3b & 4b) and $\varepsilon = 0.05$ (Fig. 3a & 4a). The impact of surface porosity on the concentration field and hence, on the flux through the film can be clearly visualized from these figures. A low porosity clearly confines the flux which may be visualized from the concentration gradients to the vicinity of the pore opening. As the porosity increases, this becomes significantly less pronounced and the entire film section is subject to significant concentration variations. Fig. 4 also shows the streamlines along with the concentration profile which indicate representative diffusive paths through the film for each case. The effect of a reduced porosity is quite apparent. With the reduction of porosity, the section of the membrane active for penetrant diffusion diminishes and becomes more restricted to the pore region. When either the thickness or porosity is substantially increased, the flux distribution within the

membrane becomes more even and the dependence on the porosity becomes smaller, which is evident from Fig. 2. For extremely low film thicknesses, the porosity plays a very important role and affects the flux across the membrane.

(a)

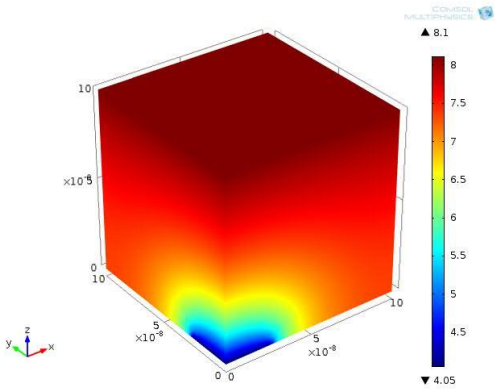

(b)

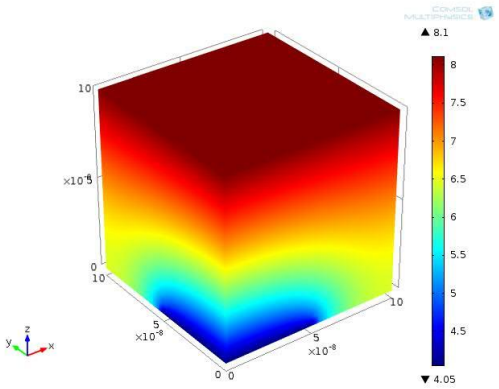

Fig.3 (a) Cut view of 3D model unit cell showing the concentration profile in the separating layer above a single pore for a support surface porosity for (a) porosity ε = 0.05 and (b) ε = 0.2

(a)

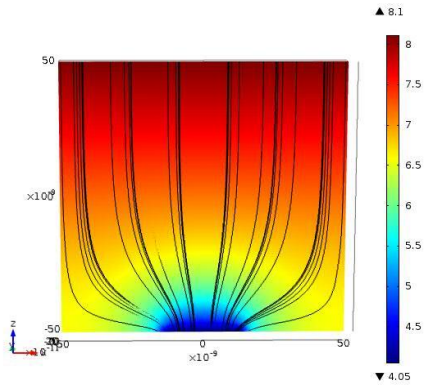

(b)

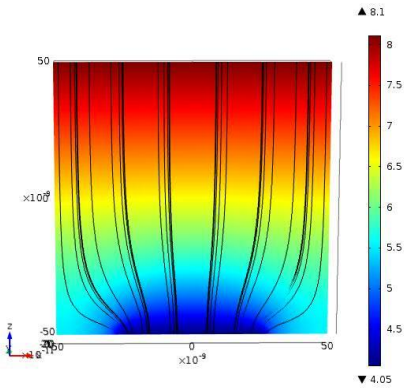

Fig.4 (a) Diffusive flow paths along with the concentration profile shown along X-Z plane at (a) $\varepsilon = 0.05$ and (b) $\varepsilon = 0.2$.

(a)

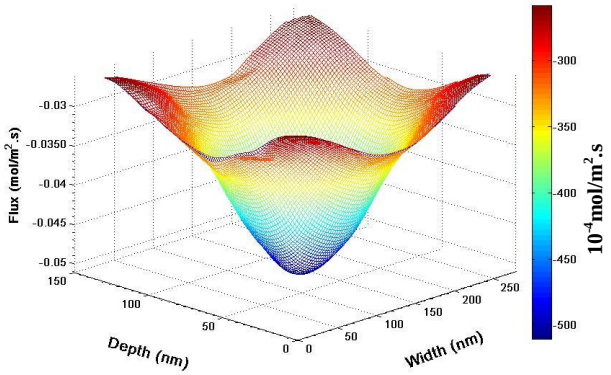

(b)

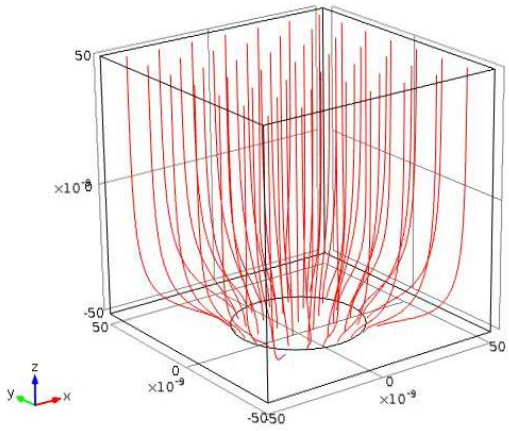

Fig.5. (a) Surface plot of diffusive mass flux at the bottom face of the cube shown in Fig. 1. (b) 3D streamlines showing the diffusive paths through the thin film.

(a)

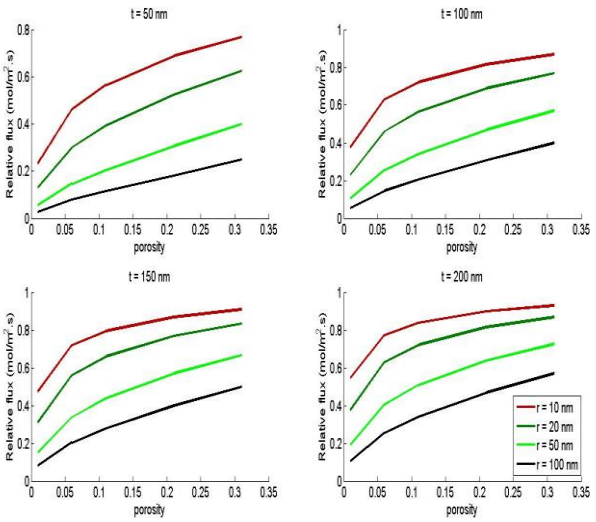

(b)

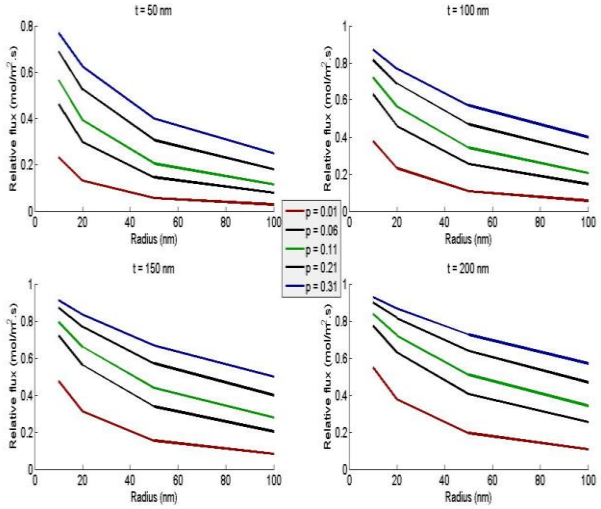

Fig. 6. Relative flux as a function of (a) porosity at a particular thickness and different radius and (b) radius at a particular thickness and different porosities.

Fig 5a shows the spatial variation in the flux at the bottom surface of the membrane. The concentration gradient peaks at the center of the pore and gradually fades away towards the edges. This is expected, since the species can diffuse perpendicularly through the separating layer and enter the support. The streamlines shown in Fig 5b represent the diffusive path of the species transporting through the coating film. It can be seen that the diffusive path for the species right above the pore is much shorter than those located towards the edges. This leads to the lateral transport of the species towards the bottom end of the film, decreasing the apparent permeance through the thin film membranes.

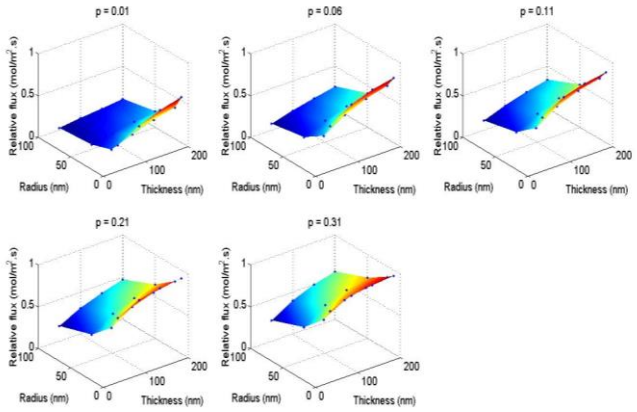

Fig. 7. Surface plots of the relative flux as a function of support geometrical parameters at various porosities.

Fig 6a indicates that the maximum permeance is attained at a lower radius for any given support porosity and thickness of the coating film. The figure confirms the general observation that the relative permeance increases as the porosity increases. The steeper gradient in the flux at low porosities and higher thickness shown in fig 6b indicate the strong dependence of the separation performance on geometrical parameters of the support membrane. From Fig 7 we can say the more pronounced effects on the flux are observed at lower porosities upon changing the geometric parameters of the membrane.

4 CONCLUSION

Modeling results indicate that the permeance of composite RO membranes strongly depends on the skin layer thickness and the pore structure of the support membrane on which the coating film is formed. The results suggest that the performance of the composite membrane can be significantly improved by adjusting the key geometrical parameters including porosity and pore size of the support membrane independent of the properties of the coating film.

REFERENCES

[1] R.W. Baker, Membrane Technology and Applications, 3rd ed., John Wiley and Sons, Ltd., Chichester, UK, 2012.
[2] L.F. Greenlee, D.F. Lawler, B.D. Freeman, B. Marrot, P. Moulin, Reverse osmosis desalination: Water sources, technology, and today's challenges, Water Res., 43 (2009) 2317-2348.
[3] M.A. Shannon, P.W. Bohn, M. Elimelech, J.G. Georgiadis, B.J. Marinas, A.M. Mayes, Science and technology for water purification in the coming decades, Nature, 452 (2008) 301-310.
[4] K.A. Lundy, I. Cabasso, Analysis and construction of multilayer composite membranes for the separation of gas mixtures, Ind. Eng. Chem. Res., 28 (1989) 742-756.
[5] G.Z. Ramon, M.C.Y. Wong, E.M.V. Hoek, Transport through composite membrane, part 1: Is there an optimal support membrane?, J. Membr. Sci., 415 (2012) 298-305.